Available online at www.sciencedirect.com
ScienceDirect
Developmental Biology 299 (2006) 594–608
DEVELOPMENTAL BIOLOGY
www.elsevier.com/locate/ydbio

Genomes & Developmental Control

Myogenic regulatory factors Myf5 and Myod function distinctly during craniofacial myogenesis of zebrafish

Cheng-Yung Lin, Rong-Feng Yung, Hung-Chieh Lee, Wei-Ta Chen, Yau-Hung Chen [1], Huai-Jen Tsai *

Institute of Molecular and Cellular Biology, National Taiwan University, Room 307, Fisheries Science Building, No. 1, Section 4, Roosevelt Road, Taipei 106, Taiwan

Received for publication 30 January 2006; revised 21 July 2006; accepted 19 August 2006
Available online 24 August 2006

Abstract

The functions of Myf5 and Myod are well known in trunk myogenesis. However, the roles that Myf5 and Myod play during craniofacial myogenesis are far from well known. We observed that zebrafish *myf5* was detected in the primordia of the obliques, lateral rectus, sternohyoideus, and pharyngeal mesoderm cores. In contrast, *myod* transcripts were expressed in all head muscle precursors at later stages. Knockdown of *myf5* revealed that Myf5 was required for the development of the obliques, lateral rectus, sternohyoideus, and all pharyngeal muscles, whereas knockdown of *myod* proved that Myod was required for the development of superior rectus, medial rectus, inferior rectus, lateral rectus, and the ventral pharyngeal muscles. *myod* mRNA did not rescue the loss of the cranial muscle caused by injecting *myf5*-morpholino, or vice versa, suggesting that the functions of Myf5 and Myod were not redundant in head paraxial mesoderm, a finding different from their functions in trunk myogenesis. Myf5, but not Myod, was required for the forward migration of *myf5*-positive oblique precursors. All evidences reveal that Myf5 and Myod function independently during cranial myogenesis. On the basis of the expression patterns of *myf5* and *myod*, we propose a model to present how Myf5 and Myod are involved in head myogenesis of zebrafish.

Keywords: Myf5; Myod; Cranial myogenesis; Zebrafish

Introduction

The paraxial mesoderm comprises the anterior (head or cephalic) mesoderm and the posterior (trunk somites and tail) mesoderm of vertebrates (Pownall et al., 2002). Unlike trunk muscle, which originates from somites, head muscle is derived from the unsegmented, nonepithelial paraxial mesoderm flanking the hindbrain and midbrain and from the prechordal mesoderm regions. Head muscle develops in two regions: branchiomeric and nonbranchiomeric (Noden, 1983; Couly et al., 1992; Trainor et al., 1994; Hacker and Guthrie, 1998; Mackenzie et al., 1998). Branchiomeric muscle includes the muscles of mastication, derived from the first or mandibular arch; the muscles of facial expression, derived from the second or hyoid arch; and the muscles of the pharynx and larynx, derived from more caudal arches (Kaufman and Bard, 1999). Non-branchiomeric head muscle includes extraocular muscles, derived from the anterior-most paraxial and prechordal mesoderm; and tongue muscles, derived from the hypoglossal cord and originating in the anterior somites (Mackenzie et al., 1998; Kaufman and Bard, 1999).

The basic helix–loop–helix myogenic regulatory factors (MRFs) play crucial functions that trigger the expression of muscle structural proteins and permit the assembly of functional myofibers (Molkentin and Olson, 1996). Myf5 and Myod direct the myogenic lineage, evidenced by the finding that double-mutant mice do not form skeletal muscle, a result of the absence of precursor myoblasts (Rudnicki et al., 1993; Kaul et al., 2000; Kablar et al., 2003). In the absence of these factors, progenitor cells remain multipotent and their cell fates can change (Tajbakhsh et al., 1996; Kablar and Rudnicki, 1999). However,

* Corresponding author. Fax: +886 2 2363 8483.
E-mail address: hjtsai@ntu.edu.tw (H.-J. Tsai).
[1] Present address: Graduate Institute of Life Sciences, Tamkang University, Taipei, Taiwan.

0012-1606/$ - see front matter © 2006 Elsevier Inc. All rights reserved.
doi:10.1016/j.ydbio.2006.08.042

in Myf5$^{-/-}$ mutants, muscles occur normally in limb and branchial arch progenitors (Kablar et al., 1997); in Myod$^{-/-}$ embryos. Skeletal muscles in trunk develop normally and Myf5 is significantly up-regulated (Rudnicki et al., 1992). Although Myod mutant embryos exhibit the delayed development of limb musculature, the limb myogenesis still keeps on processing (Kablar et al., 1997), indicating that Myod and Myf5, have functional redundancy during somitogenesis (Pownall et al., 2002). In zebrafish, embryos that received *myf5*- or *myod*-morpholino oligonucleotide (MO) alone developed somites normally (Lee et al., 2006), suggesting that *myf5* and *myod* perform complementary functions during somitogenesis. However, Kassar-Duchossory et al. (2004) state an epistatic relationship among MRFs, that is, Mrf4 acts upstream of *myod* and directs embryonic multipotent cells into the myogenic lineage. This finding contradicts the theory that myogenic identity is conferred only by Myf5 and Myod.

Several transcription factors and signaling modulators play important roles in mediating the response of signals from surrounding tissues to induce expression of MRFs during skeletal myogenesis (Borycki and Emerson, 2000; Sabourin and Rudnicki, 2000; Tajbakhsh and Buckingham, 2000). However, the finding of distinct regulatory networks of MRFs in head and in trunk myogenesis has been reported by many investigators (Patapoutian et al., 1993; Tajbakhsh et al., 1997; Hacker and Guthrie, 1998; Mootoosamy and Dietrich, 2002). Mice lacking Myf5 and the paired homeodomain transcription factor Pax3 do not develop skeletal muscle in the trunk or limb, yet head muscle forms normally (Tajbakhsh et al., 1997). Furthermore, mice lacking Capsulin and MyoR fail to express Myf5 in the first arch and lost a subset of mandibular arch-derived muscle, but trunk muscle development was not affected (Lu et al., 2002). In chick, Lbx1/Pax7/Paraxis have distinct regulatory cascades in head and in trunk myogenesis (Mootoosamy and Dietrich, 2002) and the Wnt signals, which promote trunk myogenesis, have been proven to block head myogenesis (Tzahor et al., 2003). In zebrafish cranial muscle development, *myod* expression is found only in branchiomeric muscle and extraocular muscle (Schilling and Kimmel, 1997).

Throughout vertebrate evolution, head muscle development has shown tremendous diversification (Goodrich, 1958). However, little is known about head muscle development in lower vertebrates. The epistatic relationship and the complementary effects among MRFs in muscle systems not derived from somites, such as craniofacial muscle development, have never been reported. Moreover, the role of the MRFs that are involved in head muscle development has not been elucidated. In this report, we highlight the functions of zebrafish Myf5 and Myod during cranial muscle development. Myf5 gene transcripts are detected transiently in branchial arch mesoderm cores and extraocular muscle, and inferior oblique and superior oblique primordial cells. However, when *myf5* translation is inhibited, almost all head muscle, including that derived from trunk paraxial mesoderm, is lost. On the other hand, when Myod translation is inhibited, major cranial muscles are still present, such as adductor hyomandibulae, adductor mandibulae, adductor opercula, dilator operculi, inferior oblique, levator arcus palatine, sternohyoideus, and superior oblique. We also prove that Myf5 and Myod do not have redundant functions in head paraxial mesoderm. Knockdown of Myf5 abolished the migration of cranial muscle primordia. Therefore, on the basis of the expression pattern of *myf5* and *myod*, we propose three putative pathways of how Myf5 and Myod regulate the development of craniofacial muscles.

Materials and methods

Zebrafish transgenic lines

Two transgenic lines of zebrafish, Tg(α-*actin*:RFP) and Tg(*myf5*:EGFP), were used in this study. The enhanced green fluorescent protein (EGFP) reporter cDNA in the plasmid pZα-EGFP-ITR (Hsiao et al., 2001), which contains an upstream 4-kb segment of zebrafish fast muscle α-actin fused with the EGFP reporter and flanked by an internal repeat sequence of an adeno-associated virus, was replaced by red fluorescent protein (RFP) cDNA from coral (DsRed, Clontech). The pDsRed 2-1 (Clontech) was cut first with *Not*I then with *Bam*HI after the *Not*I site was blunted. It was ligated into the pZα-EGFP-ITR vector that was cut with *Xho*I, blunted, then cut with *Bam*HI. The resultant plasmid, namely pZα-DsRed-ITR, was linearized by *Not*I and resuspended at a concentration of 25 ng/μl in double-distilled water mixed with 0.1% (v/v) phenol red prior for microinjection to generate the transgenic line Tg(α-*actin*:RFP). Parental pairs that produced RFP-positive embryos were separated and mated with wild-type individuals to confirm the putative germ-line transmitting parent. After screening, RFP-positive F1 embryos were raised to adulthood and crossed with wild-type zebrafish to generate a heterozygotic F2 generation. RFP-positive F2 individuals were then crossed with each other to generate homozygotic F3 fish, which were used to produce 100% RFP-positive F4 offspring. A similar strategy was used to generate the transgenic line Tg(*myf5*:EGFP), except that the microinjected plasmid was pZMYP-BAC80E, in which an upstream region of zebrafish *myf5* was fused with the EGFP reporter.

Knockdown of Myf5 and Myod in zebrafish embryos

Antisense MOs were designed specifically for translation inhibition of *myf5*-MO, TACGTCCATGATTGGTTTGGTGTTG, which was complementary to nucleotides (nt) 28-52, respectively, of zebrafish *myf5* cDNA (GenBank accession no. NM131576). The *myod*-MO, GTTTTTTCTACCTCAACAGCC-TATA, was complementary to nt 180–204 of zebrafish *myod* cDNA (GenBank accession no. NM131262). All oligonucleotides were prepared at a stock concentration of 1 mM and were diluted to the desired concentrations, that is, either 4, 2, or 1 ng, for microinjection into each embryo.

Fish embryos and whole-mount in situ hybridization

The procedures for zebrafish culture, embryo collection, fluorescent observation, and whole-mount *in situ* hybridization have been described previously (Lee et al., 2006), except that *myf5* (GenBank accession no. NM131576), *myod* (GenBank accession no. NM131262), *myogenin* (GenBank accession no. NM131006), *mrf4* (GenBank accession no. NM001003982), α-*actin* (GenBank accession no. AF180887), and *met* (GenBank accession no. NM001007124) were used as probes. They were digoxigenin-labeled, after we cloned their partial DNA fragments. The designation of head muscle and the developmental stage of zebrafish were following those of Schilling and Kimmel (1997).

mRNA preparation for the rescue experiment

Capped mRNAs of *myf5* and *myod* were synthesized according to the protocol of the manufacturer (Epicentre). The resultant mRNAs were diluted to 44 ng/μl and 22 ng/μl for *myf5* mRNA and *myod* mRNA, respectively, with distilled water. Approximately 2.3 nl was used in injection into one-cell stage embryos.

Time-lapse and imaging analyses

Embryos derived from the transgenic line Tg(*myf5*:EGFP) were dechorionized and anesthetized with buffered ethyl *m*-aminoboenzoate (Tricaine; Sigma). Then, embryos were transferred to 0.5% agar containing an embryo medium with 10 mM HEPES and Tricaine. Axiovert 200 M Inverted Microscope (Zeiss) was used to capture the image approximately every 20 min from 40- to 48-hpf period. Embryos were always kept at 28.5°C on the heated microscope stage during time-lapse analysis. Image analysis was processed by using MetaMorph 7.0 software (Molecular Derice).

Results

All cranial muscles are tagged with RFP in the transgenic zebrafish line Tg(α-actin:RFP)

To characterize the functions of Myf5 and Myod during head development, we generated a zebrafish transgenic line Tg(α-*actin*:RFP) that carried a DNA construct in which the RFP reporter was driven by a zebrafish fast-muscle α-actin promoter. Whole-mount *in situ* hybridization revealed that the RFP reporter gene started to transcribe at 14 h postfertilization (hpf) in the somites of embryos derived from Tg(α-*actin*:RFP), indicating that the transcription of transgenic and endogenous α-*actin* genes was initiated at the same stage (Figs. 1A, B). Red fluorescent signal was observed first in somites at 20 hpf (data not shown), and this signal appeared weaker in the newly formed somites than in the old ones (Figs. 1C, D). Similarly, α-*actin* transcripts were detected first in the head region at 36 hpf, as were RFP transcripts. However, RFP signals were observed first in all cranial muscles at 55 hpf (data not shown). After 55 hpf, all cranial skeletal muscles of this transgenic Tg(α-*actin*:RFP) fish were tagged clearly by RFP (Figs. 1E, F, G, H). We also noticed that the expression of α-*actin* in the head was similar to that of *myod*.

Expression patterns of myf5 and myod in zebrafish head muscle development

We detected the spatiotemporal expression patterns of *myf5* and *myod* from 24 through 48 hpf. At 24 hpf, *myf5* was detected in the posterior region near the eye (Fig. 2A). At 30 hpf, these *myf5*-positive cells distributed at the first branchial arch mesoderm core (Figs. 2A, B, C). In addition, *myf5* started to express in the inferior oblique (io) and lateral rectus (lr) muscle primordial cells (Fig. 2B). At 32 hpf, *myf5* was expressed not only in io and lr, but also in the muscle primordia of superior oblique (so) muscle and of the first, the second, and the third branchial arches (Fig. 2C). After 32 hpf, *myf5* transcripts rapidly were absent in the first arch and lr, but expression increased in the third branchial arch mesoderm core (Figs. 2C, E). At 36 hpf, *myf5* was expressed predominately in sternohyoideus (sh), which migrates from the anterior somites (Fig. 2E). At 36 through 48 hpf, *myf5* continued to be expressed in the muscle primordia of so, io, sh, and the mesoderm cores of the second and the third branchial arches (Figs. 2G, I). After 48 hfp, *myf5* transcripts gradually decreased in the head region.

Unlike the expression pattern of *myf5*, *myod* transcripts were detected first in the head muscle primordia of the superior rectus (sr), medial rectus (mr), and inferior rectus (ir), lr, and in the first branchial arch mesoderm core at 32 hfp (Fig. 2D). At 36 hpf, *myod* was detected in the first (masticatory plate, MP; intermandibularis, IM) and the second arch mesoderm cores (constrictor hyoideus dorsalis, CHD; constrictor hyoideus ventralis, CHV). Thereafter, these mesoderm cores were cleaved individually into dorsal (MP in the first arch; CHD in the second arch) and ventral (IM in the first arch; CHV in the second arch) areas (Figs. 2F, H, J) (Schilling and Kimmel, 1994). At 42 to 48 hpf, all the cranial muscle were *myod*-positive (Figs. 2H, J).

By comparing the expression patterns of *myf5* and *myod* in head, we found that almost all the cranial muscle expressed *myf5* in the early stages and then expressed *myod* afterward. At 32 hpf, the first arch mesoderm core was *myf5*-positive. However, when the first arch subdivided into MP and IM, the *myf5* transcripts started to decrease at 36 hpf, as in the second and third arch. The expression of *myf5* was decreased greatly after 42 hpf. Instead, *myod* became positive in these muscles at 36 hpf. A group of *myf5*-negative muscle primordia, such as mr/ir/sr, became *myod*-positive after 32 hfp (Figs. 2F, H). In addition, after we compared the spatiotemporal expressions of *myf5*, *myod*, *myogenin*, and α-*actin* in the wild-type embryos and the RFP reporter signaling in the transgenic line Tg(α-*actin*:RFP) (please see Supplemental data 1), we hypothesize that Myf5 and Myod are involved in cranial muscle development but that they play roles differently.

Functions of Myf5 and Myod in zebrafish cranial muscle development

To determine whether *myf5* and *myod* play roles during craniofacial muscle development, we microinjected MOs to knock down Myf5 or Myod specifically. When *myf5*-MO was injected into zygotes from Tg(α-*actin*:RFP) fish, only the muscle primordia of sr, mr, and ir were RFP-positive at 72 hpf (Fig. 3A vs. B), even until 7 days postfertilization (dpf; data not show); the remainder of the cranial muscle was lost in *myf5* morphants, even at 7 dpf. The transcripts of *myod* and *myogenin* were only detected in the primordia of sr, mr, and ir at 36 hpf (Fig. 3D) and 58 hpf (Figs. 3H, J) in *myf5* morphants. The MO-induced phenotypes were dose-dependent (Table 1). Next, we detected *et1* expression in *myf5* morphants to reveal whether the loss of ventral cranial muscle in *myf5* morphants was due to the abnormal development of pharyngeal ventral mesoderm cores. Results showed that the pharyngeal ventral mesoderm cores of *myf5* morphants developed normally (Fig. 3E vs. F). These results indicate that Myf5 knockdown did not affect cranial mesoderm cores development. Myf5 expression in the arch 1 and 2 mesoderm cores is necessary for initiating the further myogenesis of ventral mesoderm cores. In addition, although *myod* and *myogenin* were expressed in all cranial muscle (Figs. 3G, I), Myf5 knockdown resulted in restricting *myod* and *myogenin* expression in the primordia of sr, mr, and ir (Figs. 3H, J). Thus, we propose that Myf5 is necessary for the development of the extraocular muscles so, io, and lr, and all pharyngeal muscles.

When *myod*-MO was microinjected to specifically inhibit the translation of *myod* in the embryos derived from both wild-type

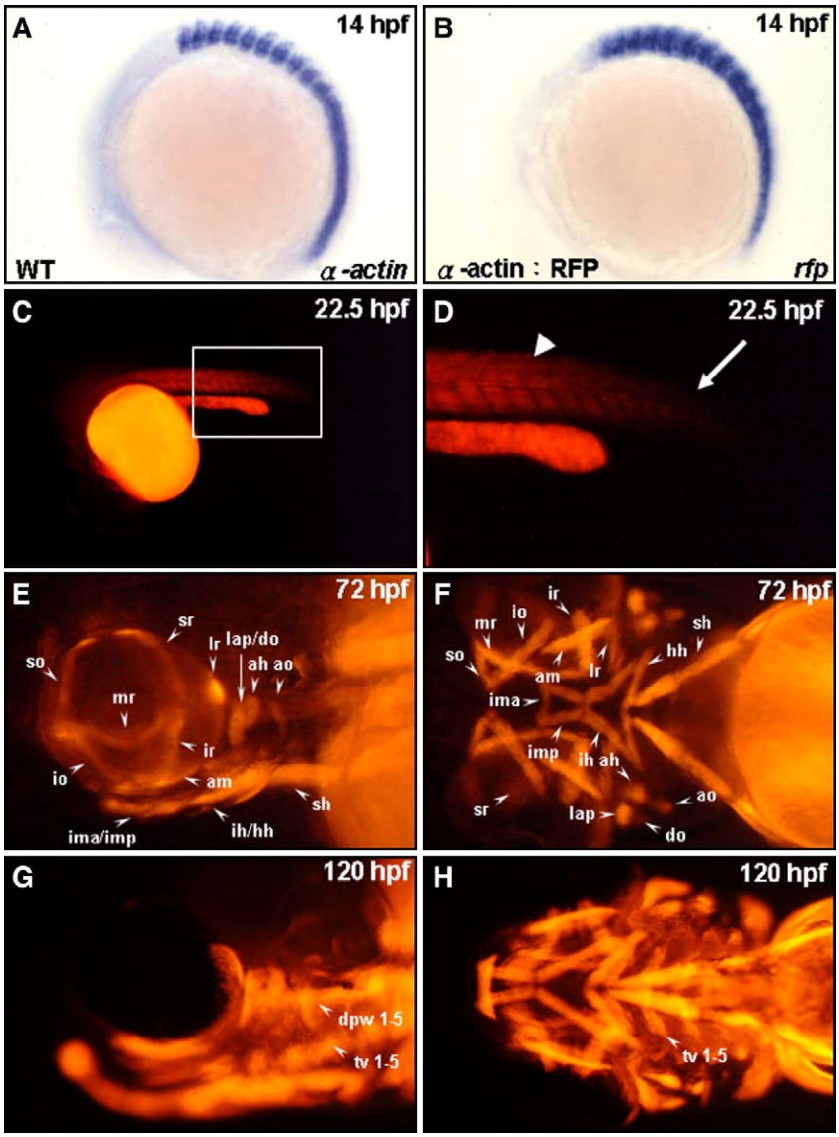

Fig. 1. Tagging all head muscles by using the transgenic zebrafish line Tg(α-*actin*:RFP). Endogenous α-*actin* transcripts (A) and red fluorescent protein (RFP) reporter transcripts (B) were detected by whole-mount *in situ* hybridization of zebrafish embryos at 14 hpf (lateral view: A, B). RFP expressions in the embryos derived from the transgenic line (α-*actin*:RFP) at 22.5 hpf (C, D), 72 hpf (E, F), and 120 hpf (G, H) were observed from a lateral view (E, G) and from a ventral view (F, H). Panel D is a magnification of panel C. RFP appeared in the formed somites (D, arrowhead) but was absent in the newly forming somite (D, arrow) at 22.5 hpf. Meanwhile, all cranial muscles were labeled by red fluorescent signal in the embryos both at 72 and at 120 hpf. The muscles are designated following the scheme of Schilling and Kimmel (1997): ah, adductor hyoideus; am, adductor mandibulae; ao, adductor operculi; do, dilator operculi; dpw1–5, dorsal pharyngeal wall 1–5; hh, hyohyoideus; ih, interhyoideus; ima, intermandibularis anterior; imp, intermandibularis posterior; io, inferior oblique; ir, inferior rectus; lap, levator arcus palatini; lr, lateral rectus; mr, medial rectus; sh, sternohyoideus; so, superior oblique; sr, superior rectus; and tv 1–5, transvs. ventralis 1–5.

and Tg(α-*actin*:RFP) fish, the RFP signals were present in the extraocular muscles so and io, and in the dorsal pharyngeal muscles, such as lap, do, ah, ao, and sh at 72 hpf (Figs. 4A vs. B, C vs. D), although the RFP signals were reduced slightly. Nevertheless, the RFP signals were lost in the extraocular muscles sr, mr, ir, and lr and in the ventral pharyngeal muscles ima, imp, ih, and hh. Moreover, the *myf5* transcripts appeared normal in *myod* morphants both at 30 hpf (Fig. 4F) and at 36 hpf (Fig. 4H), whereas the *myogenin* transcripts were expressed slightly in so, io, lap/do, am, ah, ao, and sh (Fig. 4I vs. J). Like RFP signals, neither *myf5* nor *myogenin* was expressed in the extraocular muscles sr, mr, ir, and lr and in the ventral pharyngeal muscles ima, imp, ih, and hh in *myod* morphants. The red fluorescent signal was too weak to be observed in the primordia of am in *myod* morphants before 72 hpf, but *myogenin* was detected by using whole-mount *in situ* hybridization, supporting the theory that *myogenin* was expressed in the promordia of am. However, neither the RFP signal nor *in situ*hybridization was detected in sr, mr, ir, lr, ima, imp, ih, and hh, even until 7 dpf (data not shown). The phenotypes induced by MO treatment were dose-dependent (Table 2). Again, these results suggest that the absence of cranial muscle in the *myod* morphants was *myod*-specific, not due to the delay of development in the MO-treated embryos. Although *myod* was expressed in all cranial muscles, *myod* knockdown did not affect the expression of *myf5* in so, io, dorsal arch, and sh (Figs. 4F, H), but *myogenin* transcript and the RFP-labeled muscle

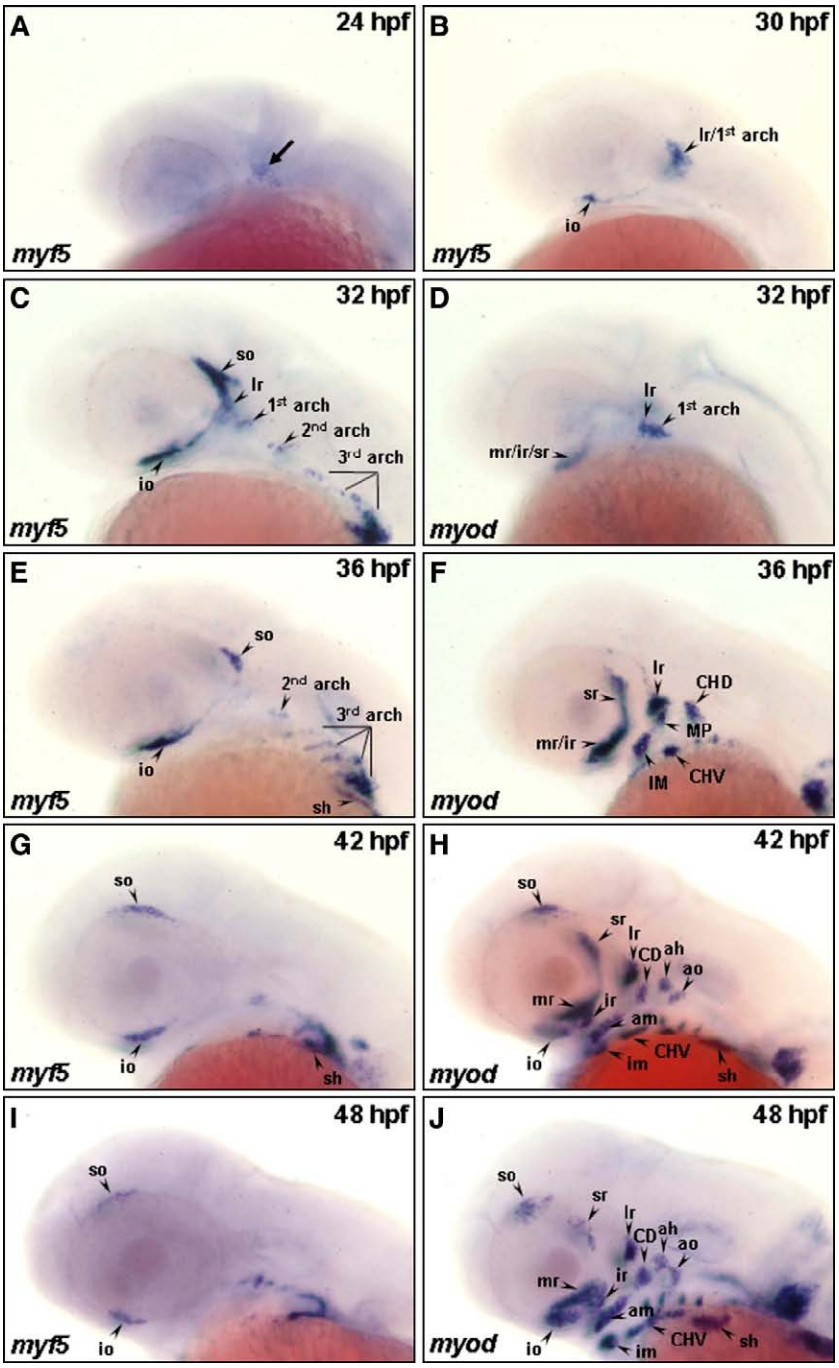

Fig. 2. The temporal expressions of *myf5* and *myod* during cranial muscle development. The temporal expressions of *myf5* (A–C, E, G, I) and *myod* (D, F, H, J) transcripts were analyzed by whole-mount *in situ* hybridization in zebrafish embryos. The transcript of *myf5* was detected in the craniofacial region at 24 hpf (A, arrow); in the io, the precursor of lr, and 1st arch (lr/1st arch) at 30 hpf (B); in the so, io, lr, 1st, 2nd, and 3rd arches at 32 hpf (C); in the so, io, sh, 2nd, and 3rd arches at 36 hpf (E); and in the so, io, and sh at 42–48 hpf (G, I). *myf5* was not expressed in the lr and 1st arch at 36 hpf (E). Meanwhile, *myod* was expressed in the craniofacial muscles mr/ir/sr, lr, and 1st arch at 32 hpf (D); in the mr/ir, sr, lr, MP, IM, CHD, and CHV at 36 hpf (F); and in all the cranial muscle at 42–48 hpf (H, J). CD: the constrictor dorsalis, which differentiates to lap and do; CHD: the constrictor hyoideus dorsalis, which differentiates to ah and ao; CHV: the constrictor hyoideus ventralis, which differentiates to ih and hh; IM: the intermandibularis, which differentiates to ima and imp; MP: the masticatory plate, which differentiates to CD and am. lr, lateral rectus; for other abbreviations, see the legend of Fig. 1.

fibers were reduced, indicating that Myod helped to enhance the myogenesis of the head muscles so, io, lap, do, am, ah, ao, and sh. Myod is required for the development of the extraocular muscles sr, mr, ir, and lr and the ventral pharyngeal muscles ima, imp, ih, and hh. Myf5 and Myod play their own distinct roles during cranial myogenesis of zebrafish.

Embryos that received either *myf5*- or *myod*-MO did not lose all the cranial muscle. However, when both *myf5*- and *myod*-MOs were injected into embryos derived from the transgenic line Tg(α-*actin*:RFP), all cranial muscle labeled with RFP was absent in the head region (Figs. 5A, B). We also detected the expression of *myogenin* and *myf4* in this *myf5*/*myod* morphant

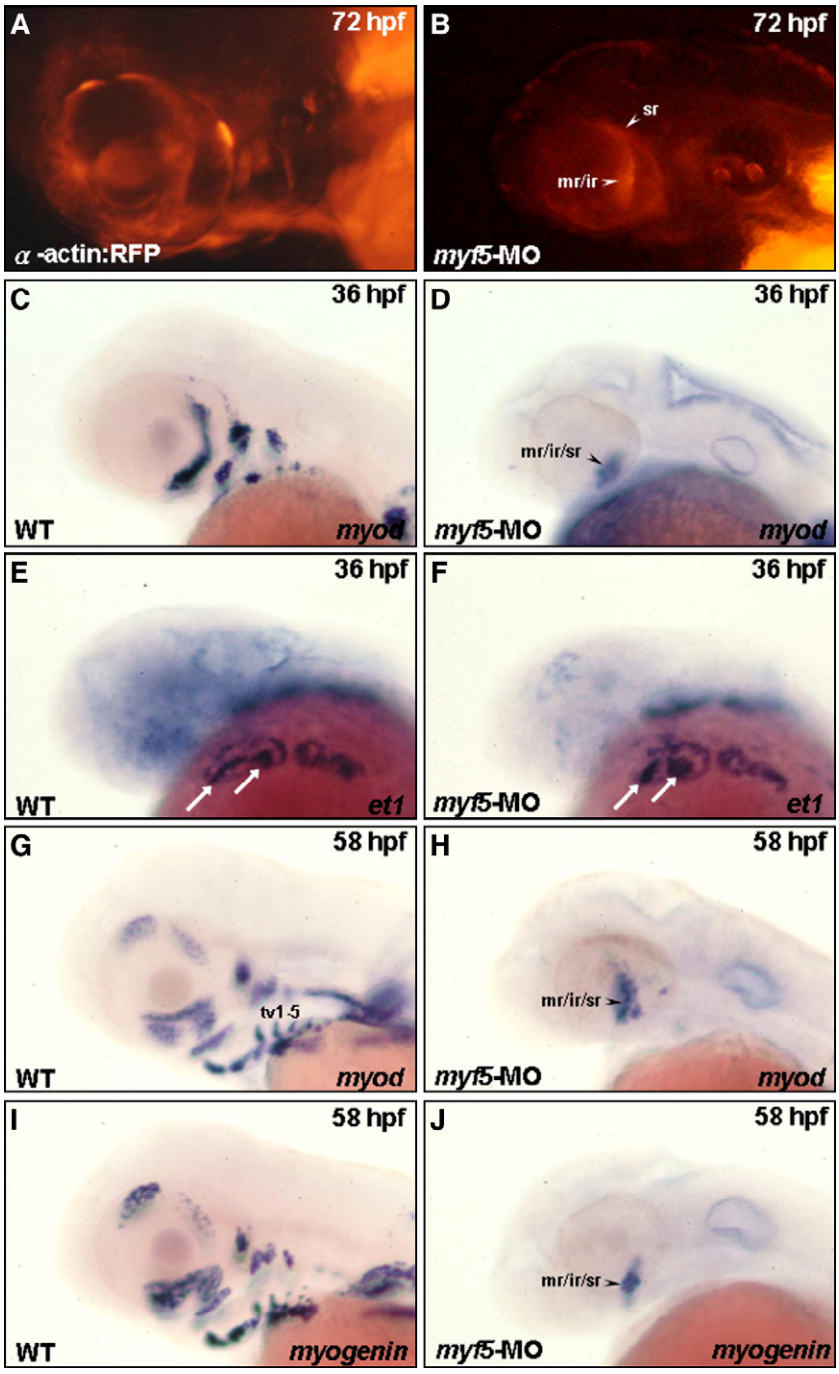

Fig. 3. Myf5 is required for cranial muscle development, except the primordia of mr/ir/sr. Embryos derived from the transgenic line Tg(α-*actin*:RFP; A, B) and from the wild-type strain (C–J) were used. All the embryos were lateral views except panels E and F, which were dorsal–lateral view. The embryos injected with 4 ng of *myf5*-morpholino oligonucleotide (MO) to inhibit *myf5* translation specifically, were studied to observe the development of cranial muscle (B) and the expression of *myod*, *et1*, and *myogenin* (D, F, H, J) at the stages indicated. Red fluorescent protein (RFP) signal was detected only in the mr/ir and sr primordia in the *myf5* transgenic morphant (A vs. B). *myod* was expressed only in the mr/ir/sr primordia in the *myf5* wild-type morphant at 36 hpf (C vs. D) and at 58 hpf (G vs. H). Similarly, *myogenin* was detected only in the mr/ir/sr primordia in *myf5* morphant (I vs. J). However, the *et1* transcript was changed little in the ventral arch mesoderm core in the *myf5* morphant (E vs. F, arrows), indicating that the development of the ventral arch mesoderm core in *myf5* morphant was normal.

and found that *myogenin* and *myf4* were not expressed in any cranial muscle (Figs. 5C vs. D, E vs. F). Furthermore, Myogenin and MRF4 did not initiate cranial myogenesis of zebrafish when both Myf5 and Myod lost their function.

To determine whether there is a redundant function between Myf5 and Myod during cranial muscle development, we co-injected *myf5*-MO with *myod* mRNAs in embryos. Interestingly, *myod* mRNA did not rescue the loss of the cranial muscle caused by *myf5*-MO: only the mr, ir, and sr were observed (Fig. 5G). When *myf5* mRNA and *myf5*-MO were co-injected, all the cranial muscles displayed a normal phenotype (Table 1). Similarly, the number of embryos displaying the normal

Table 1
myf5 is required for the development of superior oblique (so), inferior oblique (io), lateral rectus (lr), sternohyoideus (sh), and all arch muscles

myf5-MO injected concentration	so, io, lr, sh, and all arch muscle defect (%)		
	Absent	Reduced	Normal
Uninjected	0 (0/55)	0 (0/55)	100 (55/55)
0.1 ng	0 (0/44)	25 (11/44)	75 (33/44)
0.5 ng	3 (2/52)	76 (39/52)	21 (11/52)
2 ng	18 (23/73)	82 (60/73)	0 (0/73)
4 ng	85 (76/89)	15 (13/89)	0 (0/89)
4 ng+100 pg *myf5* mRNA	47 (34/72)	50 (36/72)	3 (2/72)
4 ng+50 pg *myod* mRNA	83 (79/95)	17 (16/95)	0 (0/95)

myf5-morpholino(MO)-injected defects were observed at 72 hpf embryos.

phenotype dramatically increased when *myod* mRNA was co-injected with *myod*-MO, but the defective phenotype caused by injection of *myod*-MO could not be rescued by co-injection with *myf5* mRNA (Table 2): the mr, ir, sr, lr, ima, imp, ih, and hh did not develop (Fig. 5H). Taken together, we propose that Myf5 and Myod play their own distinct roles during cranial muscle development of zebrafish.

Functions of Myf5 and Myod are not redundant in cranial myogenesis, except sh, but Myf5 and Myod are redundant in trunk myogenesis

Unexpectedly, when embryos received *myod*-MO, the expression of *myf5* in sh, which originates from anterior trunk somites (Schilling and Kimmel, 1997), was up-regulated (Fig. 6A vs. B). This consequence was consistent in the fin bud (fb) and posterior hypaxial muscle (phm), because sh, fb, and phm originate from the same migration of cells during development (Neyt et al., 2000; Haines et al., 2004).

Next, we also studied the redundant function between Myf5 and Myod in trunk in zebrafish. During trunk myogenesis, *myf5* expression in trunk was extremely slight in dorsal and ventral somites at 48 hpf (Fig. 6C), whereas *myod* expression was predominant at a low level in the trunk (Fig. 6D). However, when *myf5* was knocked down, *myod* expression was greatly enhanced in somites (Fig. 6D vs. F). Similarly, *myf5* expression in *myod* morphants was also up-regulated (Fig. 6C vs. E). The expression of *myogenin*, the downstream effector of Myf5 and Myod, was almost similar to that of *myod* but not *myf5* at 48 hpf (data not shown). Interestingly, *myogenin* appearing a weaker intensity than *myod* in wild-type was consistent with the results from *myod* morphants (data not shown). However, in *myf5* morphants, myogenin was up-regulated in the somites (Fig. 6H). Moreover, in *myod* morphants, *myogenin* was expressed strongly in the dorsal and ventral somites, which were similar to *myod* morphants of *myf5* expression at 48 hpf (Fig. 6G). This evidence strongly proves that Myf5 and Myod have a redundant function in trunk myogenesis.

Migratory cranial muscle requires myf5 but not myod

By analyzing the spatiotemporal expression of *myf5* and *myod* during cranial myogenesis, we found that both *myf5* and *myod* transcripts were observed in so, io, and sh primordia. Because the primordium of sh has been described as migratory muscle (Schilling and Kimmel, 1997), we studied migratory cranial muscle and found that not only sh but also so and io migrated from the posterior eye field toward the anterior region as the developmental stage progressed (Figs. 2C, I). The *myf5* transcripts were detected in so and io from 32 to 48 hpf, and these signals migrated from the posterior eye field toward the anterior region (Figs. 2C, E, G, I). To confirm the migration of these *myf5*-positive so and io muscles, we used the transgenic line Tg(*myf5*:EGFP), in which an upstream region of zebrafish *myf5* was fused with EGFP, to trace the migration of cranial muscle that expresses *myf5*. To analyze the spatiotemporal migration of so and io, we found that the GFP signal could be detected in so and io clearly at 36 hpf (Fig. 7A). As a later developmental stage, the GFP signal moved from the posterior eye field toward the anterior region (Figs. 7A, E, I and Supplementary Movie 1). Meanwhile, *myod* transcripts were detected first in so and io at 42 hpf, when so and io migrated at the top and bottom of the eye field, respectively (Figs. 2G, H). The spatiotemporal movement of the GFP signals in so and io was similar to the *myf5* and *myod* transcripts detected by *in situ* hybridization.

To understand whether *myf5* plays a role in cranial muscle migration, we detected the transcript of *met*, a migration cell marker (Haines et al., 2004). Results showed that the *met* transcripts were observed in both so and io of wild-type embryos at 36, 42, and 48 hpf (Figs. 7B, F, J). But the *met* signal was not detected in the embryos injected with *myf5*-MO (Figs. 7C, G, K). However, *met* was transcribed in *myod* morphants (Figs. 7D, H, L). This evidence supports the finding that *myf5* but not *myod* is required for the migration of primordial so and io.

Similar effects were also observed in other head muscles, such as sh primordium (Schilling and Kimmel, 1997). Compared with *myf5* and *myod* staining, *met* transcripts were detected in migratory cells that originated from the anterior somites, such as sh, lb, and phm primordia at 36 hpf (Figs. 8A, B, C). Knocking down the Myod level resulted in up-regulating the *myf5* expression in the primordia of sh, lb, and phm (Fig. 6B). Compared to the control embryos, the *met* transcripts were normally expressed in the sh, lb, and phm (Figs. 8C, E). However, in *myf5* morphants, the *met* signal was detected only in the phm promordia (Fig. 8D). Moreover, *myogenin* transcripts were lost in *myf5* morphants, but *myogenin* was expressed normally in *myod* morphants in the migratory muscle cells at 48 hpf (Figs. 8F, G, H). Embryos derived from the transgenic line Tg(α-*actin*:RFP) were also used to support this finding. RFP signal was lost in sh, fb, and phm in *myf5* morphants (Figs. 8I vs. J), but RFP signal was observed in *myod* morphants (Figs. 8I vs. K). Taken together, this evidence leads us to believe that *myf5* has an important role in cranial muscle migration.

Discussion

In vertebrates, presomitic and somitic multipotential mesodermal cells give rise to myogenic progenitor cells (also known as premyogenic cells), which commit to form the skeletal

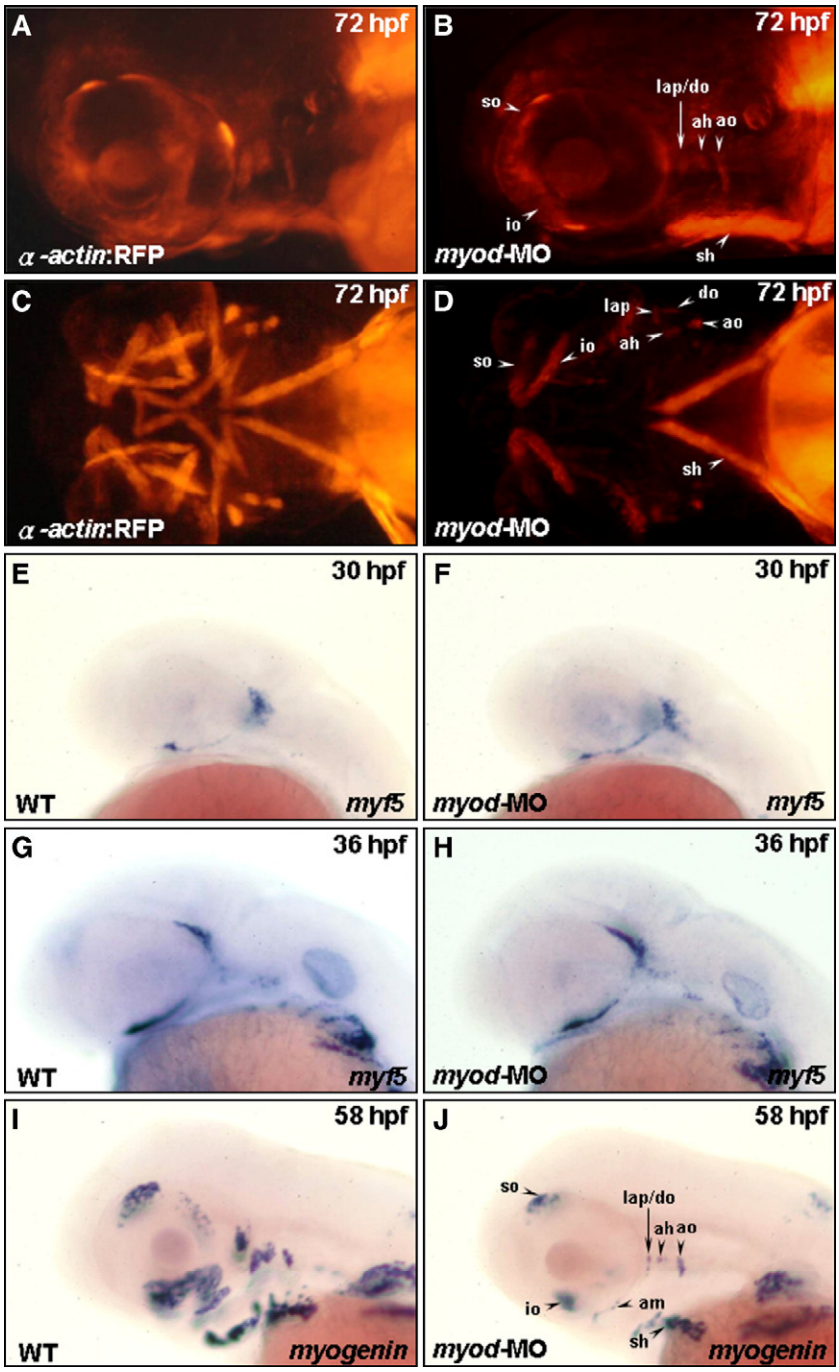

Fig. 4. Myod is required for the development of posterior extraocular recti and ventral branchial muscles. Embryos derived from the transgenic line Tg(α-*actin*:RFP) (A–D) and from the wild-type strain (E–J) were used. Embryos injected with 4 ng of *myod*-morpholino oligonucleotide (MO) to inhibit specifically *myod* translation were followed to observe the development of cranial muscle (B, D) and the expression of *myf5* (F, H) and *myogenin* (J; lateral views: A, B, E–J; ventral views: C, D) at the stages indicated. The anterior extraocular recti (io and so), dorsal branchial muscle (ah, ao, do, and lap), and sh developed normally in the *myod* transgenic morphant (A vs. B; C vs. D). The posterior extraocular (sr, mr, ir, and lr) and the ventral branchial muscle (ima, imp, ih, and hh) were totally lost. When wild-type embryos were injected with *myod*-MO, *myf5* was expressed normally in the *myod* morphants at 30 hpf (E vs. F) and at 36 hpf (G vs. H). Whereas, the expression of *myogenin* was decreased in *myod* morphants at 58 hpf (I vs. J), indicating a reduction in *myogenin*-positive muscle fibers.

muscles of the trunk, limbs, and head. Meanwhile, the more anterior nonsomitic paraxial and prechordal head mesoderm is the source of some head muscles (reviewed by Wachtler and Jacob, 1986; Christ and Ordahl, 1995). The migration of paraxial mesoderm to the branchial arches contributes precursors that develop into facial muscles in chicks (Hacker and Guthrie, 1998; Noden et al., 1999). Like other vertebrates, zebrafish cranial muscles originate from the paraxial mesoderm (Kimmel et al., 1990; Noden, 1983). Muscles that originate from the paraxial mesoderm of the first and second pharyngeal arches develop the dorsal (lap, do, am, ah, ao) and the ventral (ima, imp, ih, hh) portions of cranial muscles.

Table 2
myod is required for the development of superior rectus (sr), medial rectus (mr), inferior rectus (ir), lateral rectus (lr), and ventral arch muscles

myod-MO injected concentration	sr, mr, ir, lr, and ventral arch muscle defect (%)		
	Absent	Reduced	Normal
Uninjected	0 (0/117)	0 (0/117)	100 (117/117)
0.1 ng	0 (0/93)	2 (2/93)	98 (91/93)
0.5 ng	5 (4/74)	81 (60/74)	14 (10/74)
2 ng	61 (61/100)	36 (36/100)	0 (0/100)
4 ng	86 (51/59)	14 (8/59)	0 (0/59)
4 ng+100 pg *myod* mRNA	41 (39/96)	55 (53/96)	4 (4/96)
4 ng+50 pg *myf5* mRNA	85 (60/71)	15 (11/71)	0 (0/71)

myod-morpholino(MO)-injected defects were observed at 72 hpf embryos.

Myf5 and Myod play crucial functions to trigger the expression of muscle structural proteins and finally to permit the assembly of myofibers (Molkentin and Olson, 1996; Buckingham, 2001). Tajbakhsh et al. (1997) reported that Pax3 and Myf5 of mice follow two distinct myogenic pathways and that Myod acts genetically downstream of these genes for myogenesis in trunk muscle development; Myf5 and Myod regulate the head muscle formation independently. The regulation of *myf5* is markedly different from that of *myod*. Obviously, more detailed knowledge about the functions of Myf5 and Myod on cranial muscle development is needed.

In this study, we provide strong evidence to show the distinct roles that Myf5 and Myod play during craniofacial muscle development of zebrafish. In the *myf5*-knockdown morphants, the development of all the cranial muscles, except sr, mr, and ir, was impeded severely. The primordia of sr, mr, and ir developed normally in the *myf5* morphants. Furthermore, *in situ* hybridization also proved that *myf5* was not transcribed in sr,

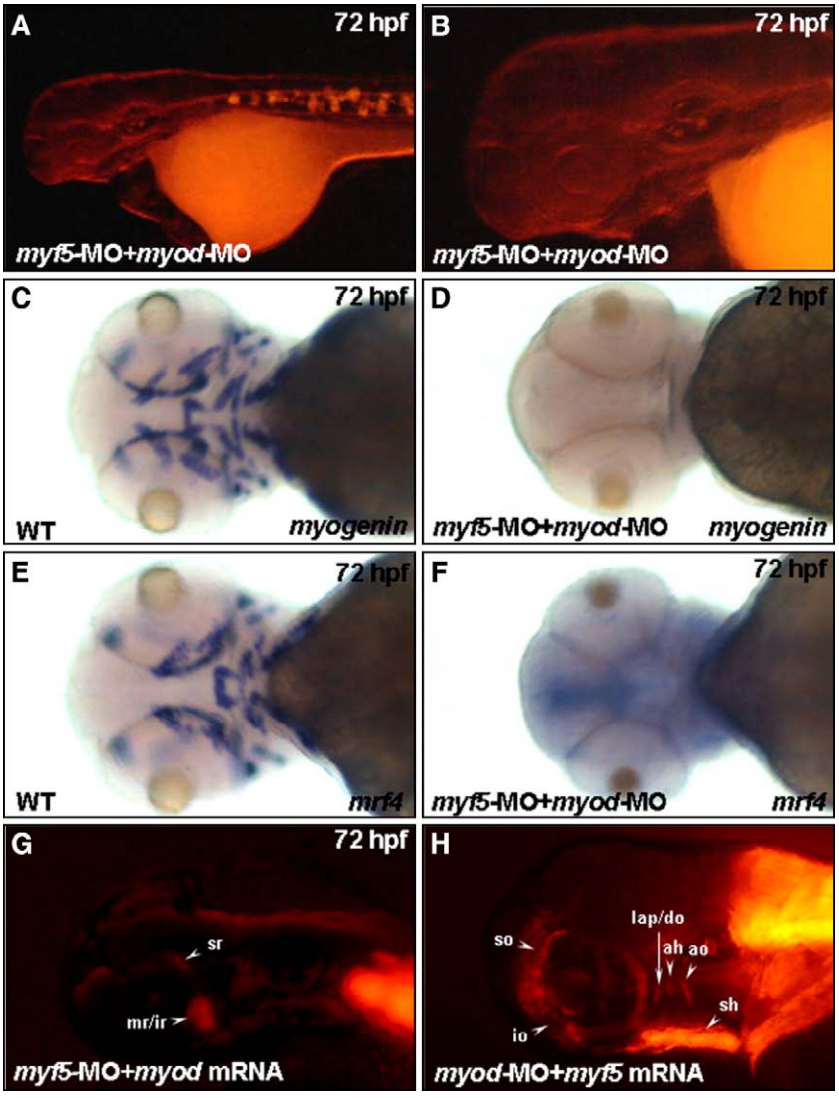

Fig. 5. Myf5 and Myod function independently to activate progenitor lineages in muscles of the head region. Embryos co-injected with 4 ng of *myf5*-morpholino oligonucleotide (MO) with 4 ng of *myod*-MO to inhibit specifically both *myf5* and *myod* translation, respectively, were used to observe the development of cranial muscle (A, B) and the expression of *myogenin* and *mrf4* (D, F) at 72 hpf. Panel B was magnified from the head area of panel A. No red fluorescent protein (RFP) signal was detected in muscle primordia in the *myf5* and *myod* double-knockdown morphants derived from the transgenic line Tg(α-*actin*:RFP; A, B). Similarly, the transcripts of *myogenin* (C vs. D) and *mrf4* (E vs. F) were not detected in the *myf5* and *myod* double-knockdown morphants (I vs. J). The *myod* mRNA did not rescue the formation of RFP-labeled primordia muscles in *myf5* morphants (G). Similarly, the *myf5* mRNA did not rescue the formation of RFP-labeled primordia muscle in *myod* morphants (H). For abbreviations, see the legend of Fig. 1.

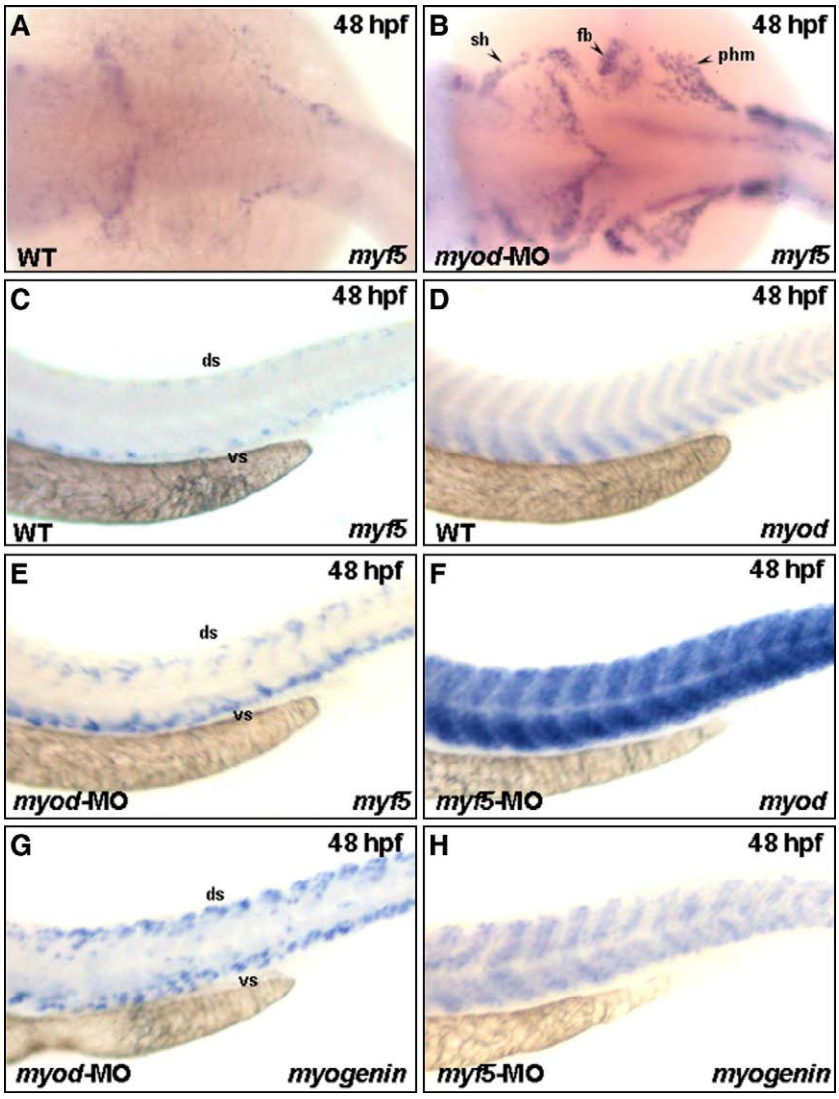

Fig. 6. Loss of Myod up-regulated Myf5 expression, and vice versa, in the cranial muscle that migrated from the anterior somites. The expression of *myf5* was increased in sternohyoideus (sh) primordia, fin bud (fb), and posterior hypaxial muscle (phm) that migrated from the anterior somites, when embryos received *myod*-morpholino oligonucleotide (MO; vs. B). This consequence was consistent in trunk myogenesis. There was weak *myf5* expression in the trunk of wild-type embryos at 48 hpf (C). However, *myf5* appeared predominantly in the dorsal (ds) and ventral (vs) parts of somites in the *myod* morphants (E), indicating that *myod* knockdown up-regulated the expression of *myf5* both in sh, which originated from trunk somite, and in trunk muscle. Similarly, the expression of *myod* was also enhanced in the trunk of *myf5* morphants, compared to wild-type embryos (D vs. F). The *myogenin* expression was similar to that of *myf5* in *myod* morphants (E, G) and to that of *myod* in *myf5* morphants (F, H).

mr, and ir. On contrast, few cranial muscles, such as sr, mr, and ir, and the ventral set of muscles (ima, imp, ih, and hh) were totally lost in the *myod*-knockdown morphants, suggesting that Myf5 and Myod may function independently and distinctly in some cranial muscles during zebrafish embryogenesis. The embryos injected with either *myf5*- or *myod*-MO in this study could survive more than 8 days. Thus, we conclude that the MO-induced phenotypes are specific.

Regulatory networks of Myf5 and Myod during cranial myogenesis are intricate

Myf5 and Myod are indispensable for cranial muscle development of zebrafish, because Myf5 or Myod have its own role without being redundant. Based on the expression patterns of *myf5* and *myod*, there are three different regulatory mechanisms of all craniofacial myogenesis (Fig. 9).

During cranial muscle development, the arch I and II mesoderm cores are subdivided into dorsal and ventral mesoderm cores. The dorsal mesoderm cores are the precursor of lap, do, am, ah, and ao, whereas the ventral mesoderm cores are the precursors of ima, imp, ih, and hh. We find that both *myf5* and *myod* are detected in the dorsal mesoderm cores, but only *myod* is expressed in the ventral groups. On the basis of data shown in this study, we propose two regulatory pathways (Fig. 9C): in pathway I, Myf5 *per se* is capable of initiating myogenesis. Once Myf5 is expressed, the expression of *myod* starts to increase, and then myogenesis proceeds further. This finding is illustrated by the expression of the muscle differentiation marker *myogenin*: *myod* and downstream

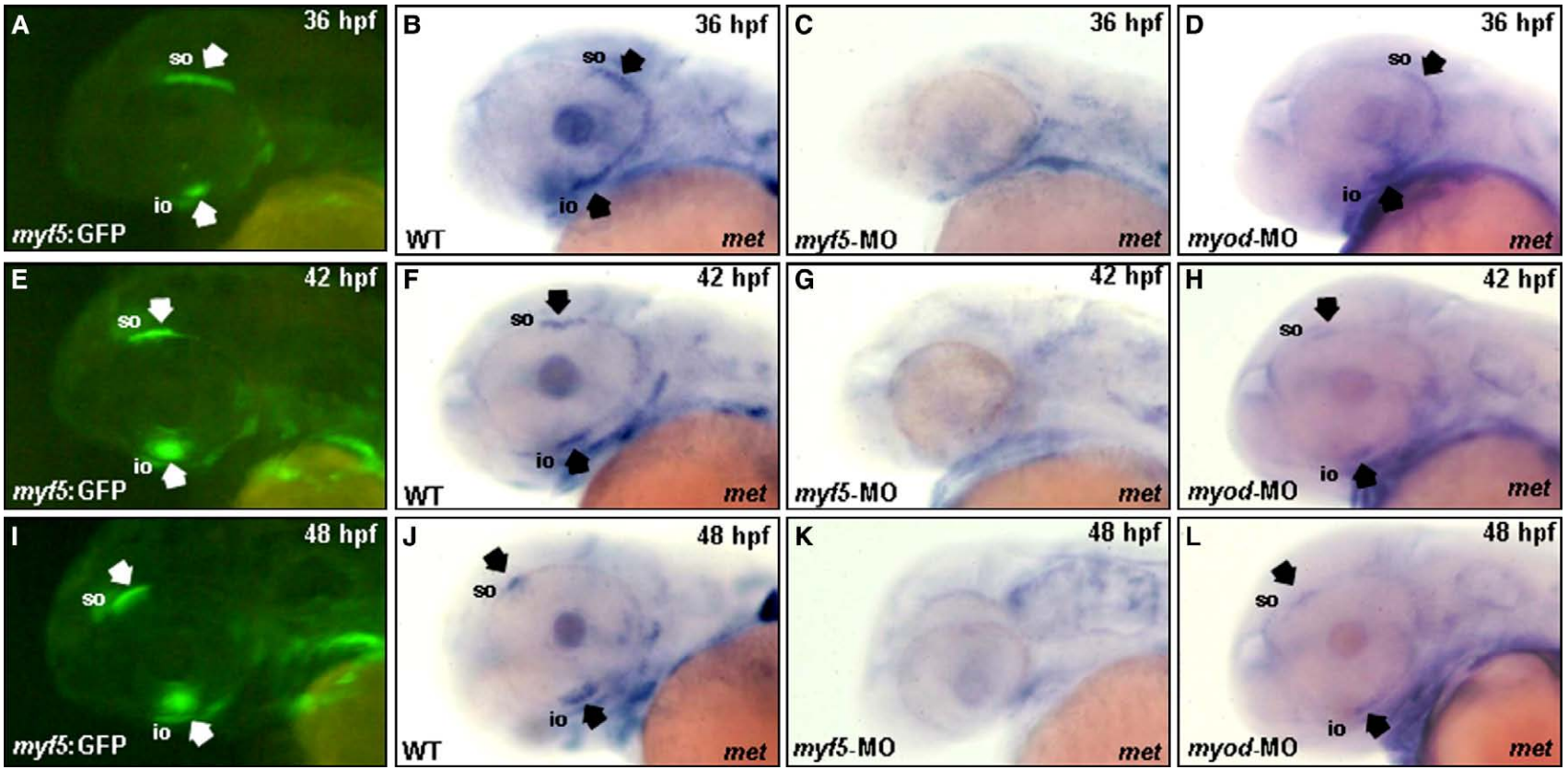

Fig. 7. Myf5 is required for the forward migration of the superior oblique (so) and inferior oblique (io) primordia toward the anterior eye region. Embryos derived from the transgenic line Tg(*myf5*:EGFP), in which an upstream region of zebrafish *myf5* was fused with enhanced green fluorescent protein (EGFP), were used to trace the migration of cranial muscle that express *myf5*. The primordia of io and so labeled with EGFP were clearly visible in the embryos derived from the transgenic line Tg(*myf5*:EGFP) at 36–48 hpf under fluorescent microscopy (A, E, I; arrows). Whole-mount *in situ* hybridization of wild-type zebrafish embryos showed that the expression of *met*, a cell marker of migration, was positive in the io and so at 36–48 hpf (B, F, J; arrows). Embryos injected with *myf5*-morpholino oligonucleotide (MO) and *myod*-MO to inhibit *myf5* and *myod* translations, respectively, expressed *met* at the stages indicated. The *met* transcript was not expressed in the io and so of *myf5* morphants (C, G, K), but *met* was expressed normally in the io and so of *myod* morphants (D, H, L; arrows). For abbreviations, see the legend of Fig. 1.

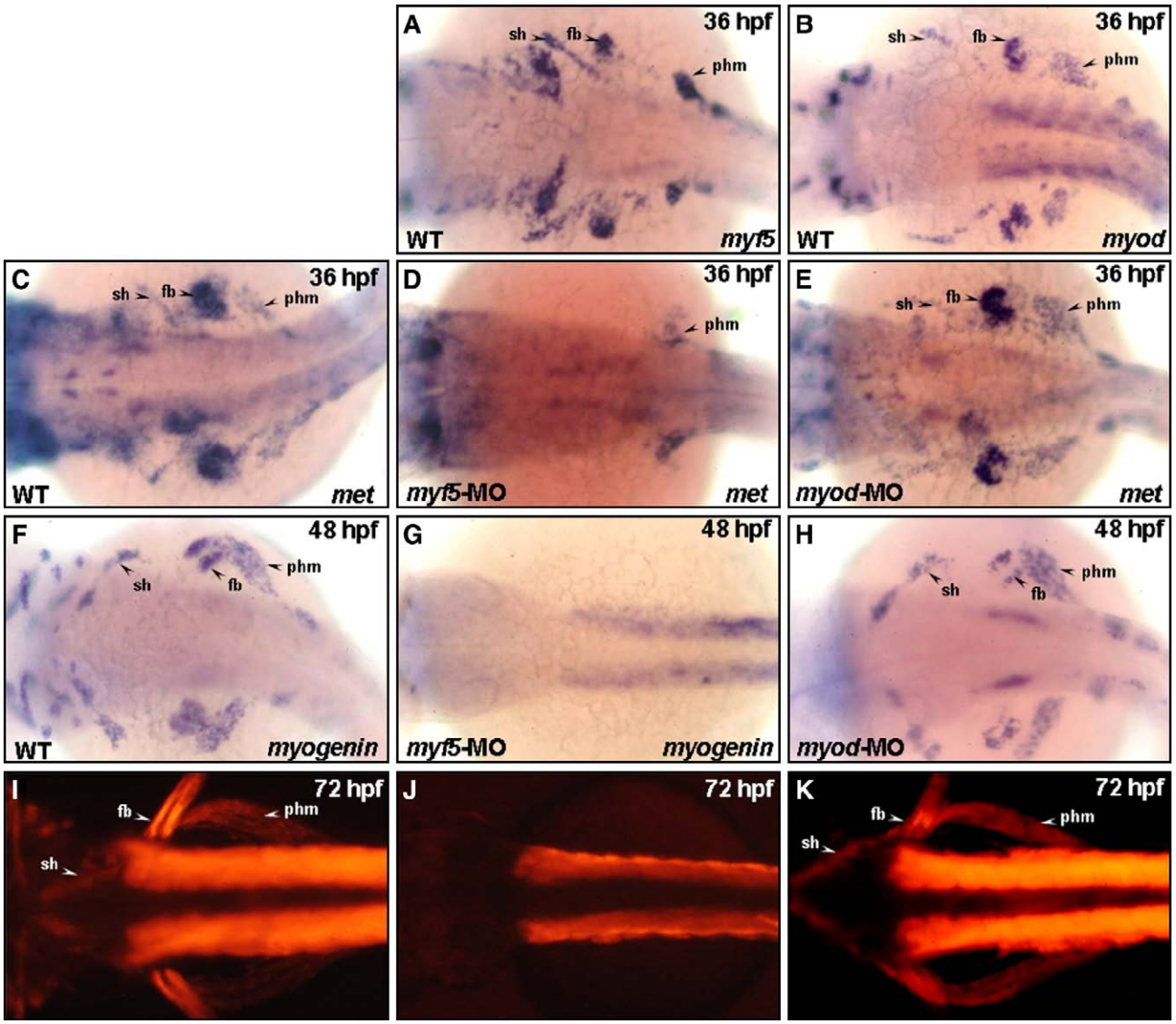

Fig. 8. Myf5 is required for the migration of the sternohyoideus (sh) primordia from anterior somites. The transcripts of *myf5* (A), *myod* (B), and *met* (C) were detected in sternohyoideus (sh) premordia, fin bud (fb), and posterior hypaxial muscle (phm), that were derived from anterior somites at 36 hpf. Embryos injected with *myf5*-morpholino oligonucleotide (MO) and *myod*-MO to inhibit specifically *myf5* and *myod* translations, respectively, expressed *met* at the stages indicated. The expression of *met* was almost lost in *myf5* morphants; only slight signals were detected in the phm (D; arrow). However, *met* was expressed normally in *myod* morphants (E). At 48 hpf, *myogenin* was expressed in the sh, fb, and phm of wild-type (F) and *myod* morphants (H), but *myogenin* was not expressed in the sh, fb, or phm of *myf5* morphants (G). Instead, the expression of *myogenin* was up-regulated in the trunk of *myf5* morphants. Embryos derived from the transgenic line Tg(*α-actin*:RFP; I–K) were used. At 72 hpf, the sh, fb, and phm showing red fluorescent signal were clearly observed both in wild-type (I; arrow) and *myod* morphants (K; arrow) but not in *myf5* morphants (J). For abbreviations, see the legend to Fig. 1.

myogenin were not expressed in the dorsal mesoderm cores of the *myf5* morphants (Fig. 3). In contrast, *myogenin* transcripts are detected in the primordia of *myod* morphants (Fig. 4), suggesting that dorsal arch muscle development of cranial myogenesis does not initiate in the absence of Myf5. However, knockdown of *myod* does not impair myogenesis, because the downstream differentiation marker *myogenin* is still expressed in these muscles, although myogenesis proceeds less efficiently. The alternative pathway for regulating the arch mesoderm core is Pathway II: muscle primordia subdivided from the *myf5*-positive core are initiated to undergo myogenesis by Myod. We find that ima, imp, ih, and hh are lost in both *myf5* morphants and *myod* morphants. These results indicate that both *myf5* and *myod* are necessary for ventral core mesoderm to undergo myogenesis.

Unlike in the arch mesoderm core, the development of extraocular muscles is regulated by three different pathways (Fig. 9C). Although both *myf5* and *myod* transcripts were detected in io and so, the primordia of io and so are lost in the *myf5* morphants but not in the *myod* morphants, indicating that Myf5 and Myod modulate the development of the extraocular muscles io and so through Pathway I. On the other hand, lr is lost in the *myf5* and *myod* morphants, suggesting that Myf5 and Myod modulate the development of the extraocular muscles lr through Pathway II. In the development of sr, mr, and ir; however, *myod* transcript is expressed but not *myf5* transcript.

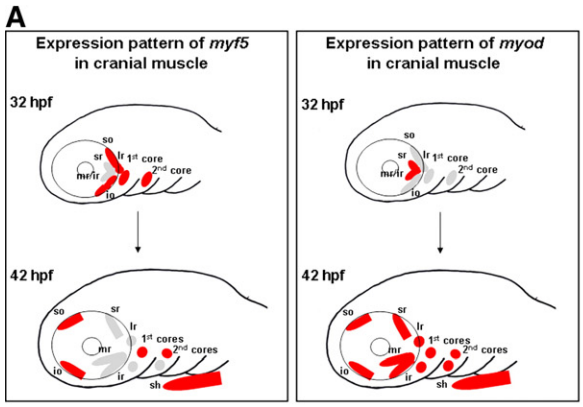

C

Muscle		Pathway	Muscle		Pathway
Pharyngeal Muscles			Extraocular Muscles		
adductor hyoideu	(ah)	I	inferior oblique	(io)	I
adductor mandibulae	(am)	I	inferior rectus	(ir)	III
adductor operculi	(ao)	I	lateral rectus	(lr)	II
dilator operculi	(do)	I	medial rectus	(mr)	III
hyohyoideus	(hh)	II	superior oblique	(so)	I
interhyoideus	(ih)	II	superior rectus	(sr)	III
intermandibularis anterior	(ima)	II			
intermandibularis posterior	(imp)	II	Trunk Migrate Muscle		
levator arcus palatini	(lap)	I	sternohyoideus	(sh)	I

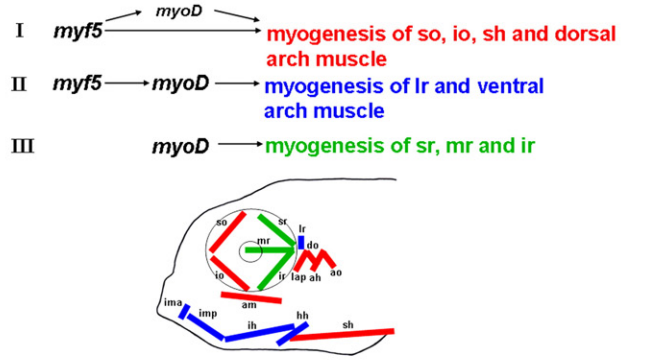

Fig. 9. A plausible model to present the distinct modulation of Myf5 and Myod during craniofacial myogenesis of zebrafish. (A) Schematic illustration of the dynamic expression of *myf5* and *myod* in the cranial muscle of zebrafish embryos at 32 and 42 hpf. The *myf5*- or *myod*-positive muscle fibers are labeled in red; *myf5*- and *myod*-negative ones are labeled in gray. (B) Schematic illustration of the presence (red) or absence (gray) of cranial muscle fibers in the embryos injected with either *myf5*-morpholino oligonucleotide (MO; left) or *myod*-MO (right) at 72 hpf. (C) Schematic diagram of all cranial muscles that are categorized into three groups (represented in red, blue, and green) on the basis of three regulatory pathways of *myf5* and *myod* during development: (I) for so, io, sh, and dorsal arch, not only does *myf5* modulate myogenesis directly to generate myogenesis at the basal level but *myf5* also triggers *myod* expression to enhance myogenesis at a high level; (II) for lr and ventral arch, *myf5* defines the cell fate of muscle and *myod* is the major factor of myogenesis; and (III) for sr, mr, and ir, *myod* modulates myogenesis directly.

This result is also supported by tracing the GFP signal from the transgenic line that carries the upstream region of zebrafish *myf5* fused with GFP reporter (Fig. 7). Thus, it is Myod but not Myf5 that modulates the development of the muscle primordia of sr, mr, and ir through Pathway III.

On the other hand, the primordia of sh, which originates from the anterior somites, was lost in the *myf5* morphants but not in *myod* morphants, suggesting that sh is modulated through Pathway I. Thus, it is worthwhile to study whether other factors are involved for controlling the development of all cranial muscles.

Myf5 and Myod function differently for craniofacial and for trunk myogenesis

Myf5$^{-/-}$ and Myod$^{-/-}$ mutant mice are viable and fertile (Kaul et al., 2000, Rudnicki et al., 1992). However, Myf5/Myod null embryos do not form skeletal muscles and die at birth because of respiratory failure (Rudnicki et al., 1993). Thus, Myf5 and Myod function redundantly for skeletal myogenesis. However, unexpectedly, we found that this redundancy present for trunk myogenesis is not the case for cranial myogenesis in zebrafish, as evidenced by co-injection of *myf5*-MO with *myod* mRNA not rescuing the *myf5*-MO-induced phenotype (Fig. 5G). Similarly, co-injected *myod*-MO and *myf5* mRNA did not rescue the defects caused by *myod*-MO (Fig. 5H). Therefore, we reason that the functions of Myf5 and Myod are not redundant in cranial myogenesis. Nevertheless, the cranial muscle sh, which originates from trunk paraxial mesoderm, is an exception to this rule. The expression of *myf5* in sh is up-regulated in the *myod* morphants (Fig. 6B), suggesting that the primordium of sh progresses as does trunk myogenesis, even when they migrate into the head region. This finding also indicates that Myf5 and Myod indeed have different regulatory mechanisms between head and trunk paraxial mesoderm, suggesting that cranial myogenesis is governed by a head-specific regulatory cascade, which is fundamentally distinct from the regulatory cascade in the trunk.

Myf5 and Myod function distinctly during development of the dorsal and ventral cranial muscles

In this study, MO-knockdown of Myf5 level results in loss of all cranial muscles, except sr, mr, and ir, suggesting that Myf5 is a key modulator during cranial muscle development. Although Schilling and Kimmel (1997) reported that *myod* is expressed in all cranial muscles of embryos in zebrafish, loss of Myod function actually does not impede the development of certain cranial muscle fibers, such as ah, am, ao, do, io, lap, sh, and so (Fig. 4). It is highly likely that Myod is required for the specification of the ventral cranial muscles but definitively not for the dorsal ones. On the other hand, Barrallo-Gimeno et al. (2004) reported that, in the mutant *mobm*^{610}/*tfap2a*, am is present but lap and do are absent and suggested that *tfap2a* is

necessary for the specification of the dorsal cranial muscles but not for the ventral ones. Thus, we propose that Myf5 may be a key modulator to control the development of major cranial muscles, whereas Myod and Tfap2a may be key modulators to control the development of the ventral and dorsal cranial muscles, respectively.

Epistatic relationship of the zebrafish MRFs in cranial myogenesis

Recently, the epistatic relationship of mouse MRFs has been proposed that both Myf5 and Mrf4 act upstream of Myod to direct embryonic multipotent cells into the myogenic lineage (Kassar-Duchossory et al., 2004). However, the epistatic relationship of the MRFs in cranial myogenesis is still unclear. Our study shows that embryos co-injected with *myf5*- and *myod*-MOs lost all the cranial muscles in the head region (Figs. 5A, B). In addition, *in situ* hybridization revealed that *myogenin* and *mrf4* were not expressed in *myf5/myod* morphants (Figs. 5D, F). This evidence indicates that Myogenin and Mrf4 are not capable of initiating cranial myogenesis. We speculate that *myogenin* and *mrf4* may serve as differentiation genes.

Myf5 is required for the migration of myogenic precursor cells

In rodent, *met* null mice lost the hypaxial mesoderm derived from the migratory muscles, such as the diaphragm, tongue, limb, and associated shoulder musculature. Also, *met* served as a migratory marker (Bladt et al., 1995; Dietrich et al., 1999). In zebrafish, the primordium of the cranial muscle sh, which originates from the anterior somites, has been defined (Schilling and Kimmel, 1997). In this report, we show that the primordia of io and so migrate during cranial myogenesis (Fig. 7). Whole-mount *in situ* hybridization showed that *met* is expressed in so, io, and sh primordia (Figs. 7, 8). Interestingly, *met* transcript is lost in the *myf5* morphants, but *met* displays normally in the *myod* morphants, suggesting that *myf5* is necessary for cranial muscle primordia migration.

In the development of mouse limb, *myf5* and *myod* transcripts are not detected in the migratory muscle primordia until they migrate into the limb buds (Tajbakhsh and Buckingham, 1994; Birchmeier and Brohmann, 2000). Unlike the mouse limb, in zebrafish cranial muscle development, the migratory cells are *myf5*- and *myod*-positive, even when they undergo migration. In *Xenopus*, p38 mitogen-activated protein kinase (MAPK) regulates the expression of *Xmyf5* and affects distinct myogenic programs (Keren et al., 2005). Inhibition of *p38 MAPK* prevents the expression of *Xmyf5* but not of *Xmyod*. The ventral body wall muscles, whose migratory precursors originate in the ventral part of somites, are reduced greatly when *p38 MAPK* and *Xmyf5* are knocked down. Together, the early activation of Myf5 and Myod in frog and fish may suggest the rapidity of their early developments to produce functional muscles for swimming.

In summary, we address the functions of Myf5 and Myod during cranial muscle development in zebrafish. Myf5 and Myod play distinct roles in cranial myogenesis. A putative model that demonstrates three pathways for Myf5 and Myod function in craniofacial muscle development is proposed. In addition, the expression of *met* in morphants supports the finding that Myf5, a well-known MRF that is involved in trunk myogenesis, also controls the cranial cell migration. This article is the first report to reveal the functions of Myf5 and Myod during cranial myogenesis in zebrafish.

Acknowledgments

This work was supported by the National Science Council, Republic of China, under grand no. NSC-95-2313-B-002-067-MY2. We are also grateful to Dr. Chang-Hao Yang and Miss Shu-Chen Shen, Department of Medical Research, National Taiwan University Hospital, for helping in time-lapse analysis and molecular imaging.

Appendix A. Supplementary data

Supplementary data associated with this article can be found, in the online version, at doi:10.1016/j.ydbio.2006.08.042.

References

Bladt, F., Riethmacher, D., Isenmann, S., Birchmeier, C., 1995. Essential role for the c-met receptor in the migration of myogenic precursor cells into the limb bud. Nature 376, 768–771.

Barrallo-Gimeno, A., Holzschuh, J., Driever, W., Knapik, E.W., 2004. Neural crest survival and differentiation in zebrafish depends on mont blanc/tfap2a gene function. Development 131, 1463–1477.

Birchmeier, C., Brohmann, H., 2000. Genes that control the development of migrating muscle precursor cells. Curr. Opin. Cell Biol. 12, 725–730.

Borycki, A.G., Emerson Jr., C.P., 2000. Multiple tissue interactions and signal transduction pathways control somite myogenesis. Curr. Top. Dev. Biol. 48, 165–224.

Buckingham, M., 2001. Skeletal muscle formation in vertebrates. Curr. Opin. Genet. Dev. 11, 440–448.

Christ, B., Ordahl, C.P., 1995. Early stages of chick somite development. Anat. Embryol. 191, 381–396.

Couly, G.F., Coltey, P.M., Le Douarin, N.M., 1992. The developmental fate of the cephalic mesoderm in quail–chick chimeras. Development 114, 1–15.

Dietrich, S., Abou-Rebyeh, F., Brohmann, H., Bladt, F., Sonnenberg-Riethmacher, E., Yamaai, T., Lumsden, A., Brand-Saberi, B., Birchmeier, C., 1999. The role of SF/HGF and c-Met in the development of skeletal muscle. Development 126, 1621–1629.

Goodrich, E.S., 1958. Studies on the Structure and Development of Vertebrates. Dover Publications, New York.

Hacker, A., Guthrie, S., 1998. A distinct developmental programme for the cranial paraxial mesoderm in the chick embryo. Development 125, 3461–3472.

Haines, L., Neyt, C., Gautier, P., Keenan, D.G., Bryson-Richardson, R.J., Hollway, G.E., Cole, N.J., Currie, P.D., 2004. Met and Hgf signaling controls hypaxial muscle and lateral line development in the zebrafish. Development 131, 3869–4857.

Hsiao, C.D., Hsieh, F.J., Tsai, H.J., 2001. Enhanced expression and stable transmission of transgenes flanked by inverted terminal repeats from adeno-associated virus in zebrafish. Dev. Dyn. 220, 323–336.

Kablar, B., Rudnicki, M.A., 1999. Development in the absence of skeletal muscle results in the sequential ablation of motor neurons from the spinal cord to the brain. Dev. Biol. 208, 93–109.

Kablar, B., Krastel, K., Ying, C., Asakura, A., Tapscott, S.J., Rudnicki, M.A.,

1997. MyoD and Myf-5 differentially regulate the development of limb versus trunk skeletal muscle. Development 124, 4729–4738.

Kablar, B., Krastel, K., Tajbakhsh, S., Rudnicki, M.A., 2003. Myf5 and MyoD activation define independent myogenic compartments during embryonic development. Dev. Biol. 2, 307–318.

Kassar-Duchossory, L., Gayraud-Morel, B., Gomes, D., Rocancourt, D., Buckingham, M., Shinin, V., Tajbakhsh, S., 2004. Mrf4 determines skeletal muscle identity in Myf5:Myod double-mutant mice. Nature 431, 466–471.

Kaufman, M.H., Bard, J.B.L., 1999. The Anatomical Basis of Mouse Development. Academic Press, San Diego, pp. 60–76.

Kaul, A., Koster, M., Neuhaus, H., Braun, T., 2000. Myf-5 revisited: loss of early myotome formation does not lead to a rib phenotype in homozygous Myf-5 mutant mice. Cell 102, 17–19.

Keren, A., Bengal, E., Frank, D., 2005. p38 MAP kinase regulates the expression of XMyf5 and affects distinct myogenic programs during *Xenopus* development. Dev. Biol. 288, 73–86.

Kimmel, C.B., Warga, R.M., Schilling, T.F., 1990. Origin and organization of the zebrafish fate map. Development 108, 581–594.

Lee, H.C., Huang, H.Y., Lin, C.Y., Chen, Y.H., Tsai, H.J., 2006. Foxd3 mediates zebrafish myf5 expression during early somitogenesis. Dev. Biol. 290, 359–372.

Lu, J.R., Bassel-Duby, R., Hawkins, A., Chang, P., Valdez, R., Wu, H., Gan, L., Shelton, J.M., Richardson, J.A., Olson, E.N., 2002. Control of facial muscle development by MyoR and capsulin. Science 298, 2378–2381.

Mackenzie, S., Walsh, F.S., Graham, A., 1998. Migration of hypoglossal myoblast precursors. Dev. Dyn. 213, 349–358.

Molkentin, J.D., Olson, E.N., 1996. Defining the regulatory networks for muscle development. Curr. Opin. Genet. Dev. 4, 445–453.

Mootoosamy, R.C., Dietrich, S., 2002. Distinct regulatory cascades for head and trunk myogenesis. Development 129, 573–583.

Noden, D.M., 1983. The embryonic origins of avian cephalic and cervical muscles and associated connective tissues. Am. J. Anat. 168, 257–276.

Noden, D.M., Marcucio, R., Borycki, A.G., Emerson Jr., C.P., 1999. Differentiation of avian craniofacial muscles: I. Patterns of early regulatory gene expression and myosin heavy chain synthesis. Dev. Dyn. 216, 92–116.

Neyt, C., Jagla, K., Thisse, C., Thisse, B., Haines, L., Currie, P.D., 2000. Evolutionary origins of vertebrate appendicular muscle. Nature 408, 82–85.

Patapoutian, A., Miner, J.H., Lyons, G.E., Wold, B., 1993. Isolated sequences from the linked Myf-5 and MRF4 genes drive distinct patterns of muscle-specific expression in transgenic mice. Development 118, 61–69.

Pownall, M.E., Gustafsson, M.K., Emerson Jr., C.P., 2002. Myogenic regulatory factors and the specification of muscle progenitors in vertebrate embryos. Annu. Rev. Cell Dev. Biol. 18, 747–783.

Rudnicki, M.A., Braun, T., Hinuma, S., Jaenisch, R., 1992. Inactivation of MyoD in mice leads to up-regulation of the myogenic HLH geneMyf-5 and results in apparently normal muscle development. Cell 71, 383–390.

Rudnicki, M.A., Schnegelsberg, P.N., Stead, R.H., Braun, T., Arnold, H.H., Jaenisch, R., 1993. MyoD or Myf-5 is required for the formation of skeletal muscle. Cell 75, 1351–1359.

Sabourin, L.A., Rudnicki, M.A., 2000. The molecular regulation of myogenesis. Clin. Genet. 57, 16–25.

Schilling, T.F., Kimmel, C.B., 1994. Segment and cell type lineage restrictions during pharyngeal arch development in the zebrafish embryo. Development 120, 483–494.

Schilling, T.F., Kimmel, C.B., 1997. Musculoskeletal patterning in the pharyngeal segments of the zebrafish embryo. Development 124, 2945–2960.

Tajbakhsh, S., Buckingham, M., 1994. Mouse limb muscle is determined in the absence of the earliest myogenic factor myf-5. Proc. Natl. Acad. Sci. U. S. A. 91, 747–751.

Tajbakhsh, S., Buckingham, M., 2000. The birth of muscle progenitor cells in the mouse: spatiotemporal considerations. Curr. Top. Dev. Biol. 48, 225–268.

Tajbakhsh, S., Bober, E., Babinet, C., Pournin, S., Arnold, H., Buckingham, M., 1996. Gene targeting the myf-5 locus with nlacZ reveals expression of this myogenic factor in mature skeletal muscle fibres as well as early embryonic muscle. Dev. Dyn. 206, 291–300.

Tajbakhsh, S., Rocancourt, D., Cossu, G., Buckingham, M., 1997. Redefining the genetic hierarchies controlling skeletal myogenesis: Pax-3 and Myf-5 act upstream of MyoD. Cell 89, 127–138.

Trainor, P.A., Tan, S.S., Tam, P.P., 1994. Cranial paraxial mesoderm: regionalisation of cell fate and impact on craniofacial development in mouse embryos. Development 120, 2397–2408.

Tzahor, E., Kempf, H., Mootoosamy, R.C., Poon, A.C., Abzhanov, A., Tabin, C.J., Dietrich, S., Lassar, A.B., 2003. Antagonists of Wnt and BMP signaling promote the formation of vertebrate head muscle. Genes Dev. 17, 3087–3099.

Wachtler, F., Jacob, M., 1986. Origin and development of the cranial skeletal muscles. Biol. Anat. 29, 24–46.